Design, synthesis and biological evaluation of a novel class of anticancer agents: Anthracenylisoxazole lexitropsin conjugates

ARTICLE *in* BIOORGANIC & MEDICINAL CHEMISTRY · FEBRUARY 2009

Impact Factor: 2.79 · DOI: 10.1016/j.bmc.2008.12.056 · Source: PubMed

9 AUTHORS, INCLUDING:

Xiaochun Han
Shandong University of Traditional Chinese …
4 PUBLICATIONS **47** CITATIONS
SEE PROFILE

Chun Li
Ithaca College
12 PUBLICATIONS **57** CITATIONS
SEE PROFILE

Andrzej Joseph Paszczynski
University of Idaho
90 PUBLICATIONS **2,600** CITATIONS
SEE PROFILE

Nicholas R. Natale
University of Montana
128 PUBLICATIONS **1,069** CITATIONS
SEE PROFILE

Published in final edited form as:
Bioorg Med Chem. 2009 February 15; 17(4): 1671–1680. doi:10.1016/j.bmc.2008.12.056.

Design, Synthesis and Biological Evaluation of A Novel Class of Anticancer Agents: Anthracenylisoxazole Lexitropsin Conjugates

Xiaochun Han[‡], **Chun Li**[‡], **Michael D. Mosher**[‡,#], **Kevin C. Rider**[‡], **Peiwen Zhou**[‡], **Ronald L. Crawford**[§], **William Fusco**[§], **Andrzej Paszczynski**[§], and **Nicholas R. Natale**[*,‡,†]
Department of Chemistry, University of Nebraska - Kearney, Kearney NE 68849-1150, Department of Chemistry, and Environmental Biotechnology Institute, University of Idaho, Moscow, ID 83844, and NIH-COBRE Center for Structural and Functional Neuroscience, Department of Biomedical & Pharmaceutical Sciences, University of Montana, Skaggs Building 480, Missoula MT 59812-1522

Abstract

The synthesis and *in vitro* anti-tumor 60 cell lines screen of a novel series of anthracenyl isoxazole amides (AIMs)¥ (**22**–**33**) is described. The molecules consist of an isoxazole that pre-organizes a planar aromatic moiety and a simple amide and/or lexitropsin-oligopeptide. The new conjugate molecules were prepared via doubly activated amidation modification of Weinreb's amide formation technique, using $SmCl_3$ as an activating agent which produces improved yields for sterically hindered 3-aryl-4-isoxazolecarboxylic esters. The results of the National Cancer Institute's (NCI) 60 cell line screening assay show a distinct structure activity relationship (SAR), wherein a trend of the highest activity for molecules with one N-methylpyrrole peptide. Evidence consistent with a mechanism of action via the interaction of these compounds with G-quadruplex (G4) DNA, and a structural based rational for the observed selectivity of the AIMs for G4 over B-DNA is presented.

Keywords

Anthracene; Antitumor; G-quadruplex; Isoxazole; Pyrrole

1. Introduction

Small molecules that bind DNA have found application in medicine, notably as cancer chemotherapeutic agents.[1, 2] That these agents are also highly cytotoxic is attributed to their tendency to bind rather indiscriminately to DNA, and any beneficial effect arises from the more rapid death rates for faster replicating cancer cells.[3] Thus, it seems a reasonable proposition that agents which are able to selectively recognize specific sequences of DNA could potentially have higher therapeutic indices.[4] In fact, considerable effort has been devoted towards the conjugation of DNA binding pharmacophores in an attempt to recognize and selectively bind specific DNA sequences.[5, 6] The bulk of the focus of this work has, until recently, been on B-

¥While not a strict acronym, the designation AIM is in honor of the memory of Professor Albert I. Meyers.

*To whom correspondence should be addressed. Phone: 406-243-4132 Fax: 406-243-5228. E-mail: Nicholas.natale@umontana.edu.
‡Department of Chemistry, University of Idaho
§Environmental Biotechnology Institute, University of Idaho
#Department of Chemistry, University of Nebraska - Kearney
†Current affiliation: CSFN, University of Montana.

DNA.[7–10] While this has produced a greatly increased understanding of the principles relating to the binding of small molecules to DNA, only limited progress in the development of new chemotherapeutic agents has been achieved.

The initial rationale for our work involved the use of an isoxazole to pre-organize B-DNA binding groups and thereby increase anti-cancer efficacy.11, [12] While our initial foray into this arena met with encouraging anti-tumor activity in screens provided by the National Cancer Institute's Developmental Therapeutics Program (NCI-DTP)[13], 14 (*vide infra*), we will present evidence herein that our lead molecules did not appear to exert their bioactivity by binding B-DNA. Concurrent with our studies at this time, numerous workers recognized that non-B-DNA conformations are potentially feasible targets for anti-tumor drug development. Two prominent theories recognize the G-quadruplex (G-4) conformation of DNA as a potential molecular target. The first line of reasoning involves the inhibition of telomere maintenance via stabilization of the G-4 conformer.[7–10, 15–18] The second theory postulates that G-4 may represent an ancient off-switch for gene expression in specific oncogenes, such as *c-myc*.19 It has been argued that molecules that selectively target G-4 could plausibly have unprecedented selectivity. Proof-of-concept has emerged in the form of a G-4 binder which advanced to clinical trials as an anti-cancer agent. [49] Based on this information, we have examined systematic structural changes in our initial lead compound to test this revised hypothesis, and describe in this work the synthesis and anti-tumor activity of these compounds in the NCI-DTP 60 cell line screening protocol. The structure activity relationship (SAR) that emerges is consistent with the G-4 binding working hypothesis, and is supported by evidence of G-4 interaction from spectroscopy, telomerase inhibition assays, and electrospray mass spectrometry.

2. Chemistry

The central strategy for the preparation of the target molecules necessitated improved synthetic methodology which could overcome formidable steric encumbrance, hindrance which was required by the premise of our working hypothesis. The route to these compounds (Scheme 1) involves the initial acetylation and nitration of N-methylpyrrole (**1**). Amide bond formation between **3** and an appropriate primary amine gave rise to the expected amidopyrroles (**6** and **12**). Reduction of the nitro group allows step-wise extension of the pyrrole chain to the desired chain length.

Linkage via an amide bond of the relatively unreactive heteroaromatic amines (**7, 9, 11, 13,** and **15**) with rigid isoxazole carboxylates connected to dirigible-like aromatic moieties was accomplished using a modification of our previously reported double activation (Scheme 2). Based on this previously developed methodology,[20,21] we prepared a set of pyrrole-type lexitropsin oligopeptides possessing at least one moiety which would be protonated at physiological pH.

The series which contained two tertiary amine groups on the end of the chain were suggested by molecular modeling studies docking target molecules, (**23**–**26**), with the solid state coordinates of the G-4 DNA reported by Neidle. Such studies indicated that the two "tails" could plausibly increase the interaction of a lexitropsin-type molecule with the DNA phosphate backbones.

The amide formation between lexitropsin and 3-(9′-anthracenyl) 5-methyl 4-isoxazolecarboxylate **17** (prepared via the 1,3-cycloaddition of 9-anthracenyl nitrile oxide and the enamine of ethyl acetoacetate)[22] was achieved through doubly activated amidation12 This amidation is actually a modification of Weinreb's amidation, which has been an effective method for direct conversion from ester to amide for many years. In classical Weinreb's amidation,23 trialkyl aluminum is mixed with free primary or secondary amine to generate

dialkylaluminum amide *in situ*, which not only increases the nucleophilicity of the amine but also makes carboxylic ester group liable to be attacked.

Double activated amidation was applied after we tried typical Weinreb's amidation on the amide formation between an amino-lexitropsin and 3-(9′-antracenyl) 5-methyl 4-isoxazocarboxylic ester and obtained products in only modest yield. We had previously observed by NMR and that the ester group of 3-(9′-anthracenyl) 5-methyl 4-isoxazolcarboxylate is located proximal to the tricyclic aromatic system as evidenced by significant magnetic anisotropy.[24] This has also been supported by subsequent x-ray studies. It is a reasonable expectation that the low reactivity arises from considerable steric hindrance preventing ester group interaction with the aluminum center of Weinreb's amide. In our modified methodology, the carboxylic ester was pre-mixed with a mild Lewis acid ($SmCl_3$) to avoid a coordinative interaction with the aluminum activated amine. In order for the Lewis acid to be compatible to the existence of basic tertiary amino group of lexitropsin as well as the utilization of alkyl aluminum, mild Lewis acid lanthanide chloride was applied. No or minimum additional coordination interaction between the lanthanide center and aluminum center is required. Two decades ago, in the study of the characteristics of lanthanide coordination catalysts for polymerization, it was suggested that $SmCl_3$ and $EuCl_3$ gave the lowest coordination interaction with alkylaluminum.[25] This finding indicates that $SmCl_3$ or $EuCl_3$ may serve as ideal lanthanide Lewis acid for the doubly activated amidation.

The modified Weinreb's amidation afforded up to 80–90% yield (Scheme 2), with a variety of hindered substrates.[26,27] This method had also been previously used to prepare the bis-leitropsin **33**.[28]

3. Results and Discussion

Our work was initiated to find a compound that meets the needs of both DNA-intercalation and B-DNA's minor-groove binding and thus targets HIV.[22] It was reported that DNA minor groove binders (such as netropsin or distamycin analogues) linked with acridine showed greater binding affinity for DNA than either acridine or minor groove binders, and optimum linker length should consist of a chain of 5 atoms.[29] An isoxazole ring was then designed to tether two biologically active portions, acridine (**22**) or anthracene (**29**) and lexitropsin peptide containing polyamidopyrroles, which exhibit preference for binding to poly-AT DNA and target HIV's *tat* gene. The results from National Cancer Institute (NCI)'s anti-HIV test showed both **22** and **29** were inactive to HIV. But surprisingly, compound **29** showed slight activity against certain human tumor cells in NCI's 60 cell line screen.13،14 This intrigued us to think about its mechanism, and COMPARE30، [31] analysis with the NCI Standard Agent Database was performed. However, it did not give a significant correlation with agents of known mechanism of action (all Pairwise Correlation Coefficients were <0.5); in contrast to the good correlations usually observed for intercalating agents.

A plethora of G-quadruplex ligands have been developed as potential molecular targets for cancer chemotherapy, such as PIPER, TMPyP, 2,6-diamidoanthraquinones, and bisamido acridines, etc. 15−19،32−34 Almost all of these G-quadruplex ligands have extended planar chromophores, and π-π stacking on the G-quartet end(s) is an important factor in their binding. [19،]32−35 The anthracene moiety in **29** may serve as an analogous π–electron rich planar chromophore, and provide binding to the top stack of G-quadruplex.[35] The lexitropsin peptide moiety was presumed to bind the TTA loop of G-quadruplex.[4,5,36,37] This explanation inspired us to design a series of analogues (**23–28, 30–32**) based on **29**.

The isoxazole moiety plays a pivotal role in our working hypothesis.[38] It is a rigid linker, pre-organizing the anthracene and peptide in three dimensions, and potentially can also function

as a prodrug to deliver the bioconjugate molecule to the cellular DNA. Lexitropsin analogues were in different lengths, to test the hypothesis that given the binding site for 'n' pyrrole rings is 'n+1' base pairs long in terms of contacted base pairs,[36,37] the relationship for the n= 0–3 series should be linear and increasing for B-DNA, but in contrast for G-4-DNA would be expected to be maximum at n=1 based on our working model (*vide infra*). Furthermore, introduction of an electron-pair bearing element (Cl) or group (phenyl) may provide interaction to cations in the G-quadruplex cavity, thus preferentially enhancing binding of these compounds to G-4 DNA.

3. 1. *In Vitro* Anti-tumor Activity

Structure-activity relationship (SAR) data for the anthracenyl isoxazole amides synthesized (**23–32**) were acquired by evaluating their *in vitro* antitumor activity against NCI's 60 human tumor cell lines.[13,14,39,40] These cell lines have been derived from nine cancer types that adequately meet minimal quality assurance criteria representing leukemia, melanoma and cancers of the lung, colon, brain, ovary, breast, prostate, and kidney. The results are shown in Table 1. Several compounds were selected for re-screening by the Biological Evaluation Committee of NCI, and for those ranges are given (AIMs **23**, **29**, **30** and **32**). Since single digit micromolar is a practical measure of encouraging anti-tumor activity, we use the total number of cell lines inhibited at single digit micromolar (N in Table 1) as an additional bench mark for overall activity. We also note those cell lines for which the anti-umor efficacy was within the nanomolar regime. We started the SAR by conjugating different lengths of lexitropsin peptide derivatives (**23–32**), and anticipating higher antitumor activity as peptide length increased. Even though varying the length of peptide had a dramatic effect on antitumor potency, the anti-tumor activity of this series of molecules had no linear relationship with the length of lexitropsin peptide. Inside each series, either double tail (**23–26**) or single tail (**27–32**), compounds which had one pyrrole (n=1) moiety gave the strongest anti-tumor activity and the broadest spectrum of inhibition at single digit micro-molar (μM) GI_{50}. Compound **24**, which had GI_{50} of 3.89 μM and inhibited 44 tumor cell lines, was 3.98 and 6.30 fold more potent than **25** and **26**, which inhibited 7 and 0 cell lines, respectively. Compound **28**, which had GI_{50} as 7.94 μM and inhibited 23 cell lines, was 4.06 and 1.32 fold more potent than **27** and **29,** which inhibited 1 and 12 cell lines, respectively. This suggests the interaction of the conjugate molecule occurs with folded DNA structures possessing n+1 (two) ATT-rich bases instead of with duplex DNA's minor groove, which requires long-chained base pair recognition structure for binding. On the other hand, compound **23,** which has no pyrrole ring in the structure, has similar GI_{50} (4.57 μM) and inhibition spectrum (42 cell lines) to that of compound **24**. Both **30** and **32** had less than 2 μM GI_{50} values, and inhibited almost all the tumor cell lines tested, indicating that introduction of electron-rich substituents at C10′ of anthracene (**30** and **32**) increased antitumor potency.

An interesting phenomenon is that compounds **23**, **27**, **30** and **32** showed higher activity against some colon cancer cell lines and non-small cell lung cancer cell lines, in which the *c-myc* oncogene is implicated as a potential contributing factor (Table 1).[59] C-*myc* expression has been reported to be downregulated by G-quadruplex stabilization.[19] This implies that compounds **23**, **27**, **30** and **32** inhibit more the cells, in which *c-myc* oncogene is over expressed, by stabilizing G-quadruplex.

3.1.A. *In vivo* activity and acute toxicity—In light of the observation that the *in vitro* activity lies outside the category of adequately studied antitumor agents, the lead compound **29** was selected for the hollow fiber *in vivo* screen.[58] The total Score of 10 reflected some *in vivo* effect, however, the score usually required for further development is 20. The mouse toxicity assay indicated no acute toxicity for **29**, and the animals showed weight gain at day 14 for all three dose regimens (100, 200 and 400 mg/kg). Therefore, further studies into SAR

development to increase the efficacy (*op cit*) and understand the mechanism of action (*vide infra*) appeared warranted.

3.2. Approaches towards understanding the Mechanism of Action (MoA)

Spectroscopy with Oligonucleotides—An oligonucleotide microarray experiment was conducted wherein the effect of **29** on Calf thymus DNA and an oligonucleotide designed by Hurley, (5′-CATGGTGGTTT(GGGTTA)$_4$CCAC-3′) known to form a quadruplex in solutions of KCl and NaCl,[41] was examined. The microarray fluorescence experiment for the mixture of Calf Thymus (CT) DNA with **29** indicates a quenching of the fluorescence but shows no bathochromic shift which would be consistent with an anthracene intercalation mechanism (Figure 2).[54,55] The Hurley-Oligonucleotide experiment with **29** shows considerable quenching of the fluorescence which is consistent with a π-stacking interaction with the G-tetrad of the quadruplex structure that forms *in situ* under the experimental conditions.[56,57]

The oligonucleotide and CT-DNA solutions were prepared in a 10mM KCl solution containing a TE buffer at pH=7.0 with a final concentration of 400μg/μL. The oligonucleotide solution was hybridized using a cyanine dye (Cy3-AP3-dCTP) utilizing a 96-well plate. AIM-2 was in an aqueous 25% DMSO solution (10μM). All experiments were carried out at 37°C with oligonucleotide solutions being incubated for 5 minutes prior to printing on the slide for analysis. All spectra were taken at four excitation wavelengths (310nm, 380nm, 410nm, and 485nm) with 530nm emission. All microarray experiments were run on a GenePix 4000 microarray fluorescence scanner with 10μm resolution and a dynamic detection range of four orders of magnitude which is linear over three orders of magnitude.

An additional fluorescence experiment involving **29** with human DNA (1:1 M ratio), sans the histones, was performed(data not shown). The results of the second fluorescence experiment were an 11nm hypsochromic shift in the λ_{max} which is inconsistent with an intercalative mechanism[55] and is likely due to hydrogen bonding interactions and or salvation of **29** in the presence of the DNA. Further fluorescence-DNA-titration experiments are warranted in light of these results.

3.2.2. COMPARE Analysis[30,31,42,43]—We used **29** as a probe or seed compound in the NCI's COMPARE Algorithm to rank the similarity of responses of the 60 cell lines to the standard agent database.[13,14, 39, 40] Similarity of pattern to that of the seed is expressed quantitatively as a Pearson correlation coefficient (PCC). The results obtained with the COMPARE algorithm indicate that compounds high in this ranking may possess a mechanism of action (MoA) similar to that of the seed compound. [30,31] COMPARE works quite well for intercalating/topoisomerase II inhibitors. The top ten matches for adriamycin, with a PCC range of 0.758 to 0.950, were all topoisomerase II inhibitors. In contrast, **29** – originally thought by our group to be a potential intercalating/minor groove binder – indicted no strong correlation to any consistent MoA, with the highest PCC being a relatively weak 0.517 (Table 2). Similar COMPARE analysis of **23–26** indicated *no significant correlation with any MoA in the Standard Agent Data Base*.

3.2.3. Computation—The dihedral angle between the tricyclic planar aromatic moiety and the isoxazole from our crystallographic studies of intermediates and analogs, is in the range of 74–80°.[22, 26–8,44,45] The idealized helical pitch angle for B-DNA was estimated to be *ca*. 47.1° by Goodsell and Dickerson in their isohelical analysis of groove-binding drugs.[46,47] Therefore, we calculated the energy associated with conformational changes to this dihedral angle in order to determine whether B-DNA binding seemed plausible. The rotational barrier calculations were performed using the torsion force constraint in the Discover module.[48] The bond in question was rotated through 360 intervals (1° increments) using a force constant of

10. After each rotation, the structure was subjected to 1000 steps of minimization, or until an rms value of 0.01 was reached, using the VA09A algorithm. The results of the conformational searches were examined with the Analysis module by constructing a table of total energy verses dihedral angle. Calculations from the INSIGHT II program suggests that this energetic cost is high, precisely in the vicinity of the Helical pitch angle requisite for binding of a C-3 aromatic isoxazole to B-DNA (Table 3).

In combination with the COMPARE analysis, we felt it was prudent to consider alternatives to B-DNA as a molecular target.

3.2.4. Revision of the working hypothesis—In light of the increasingly numerous reports postulating G-4 binding as a mechanism for anti-tumor activity, and given an overall similarity of some of the salient structural features of our compounds, we conducted a number of computational studies with the G-4 coordinates available from Neidle's elegant crystallographic studies.[50–51]

In a typical example, the minimum energy structure of NSCD 694332 and quadrulex DNA[50] was calculated in a SGI INSIGHT 2000 docking study, using the cvff forcefield, and all the solution molecules (H_2O) were removed. The whole DNA molecule was constrained, the distance between first potassium and C-10 hydrogen was fixed to <4.00 angstrom. After 3000 iterations using steepest descent minimization, in most cases the drug-receptor interaction had converged to a final energy, which the program reported as consisting of separate electrostatic and VdW components. If the minimization did not reach convergence at a set number of iterations, reasonable and slight adjustments were made to the ligand structure, and minimization was repeated until a convergent structure solution was obtained.[26]

Two of the possible docking modes we considered are illustrated in Figure 2. In the first we initiated the docking with the anthracenyl moiety intercalated between the G-tetrads. During minimization, the anthracene of **29** displaced two of the guanines (in red). In the minimized structure (Figure 2a), the Isoxazole ring N is within 3 Å of the NH_2 of the guanine of the lower, intact G-tetrad. Alternatively, we considered an external stacking (Figure 2b), and in the case of analog **30** which contained a group bearing lone pairs at C(10) of the anthracenyl group, C (10) tended to orient – again after minimization – within 2.62Å over the potassium in the cavity of the G-tetrad.

Similar features which emerged from both of these minimized structures were (1) the isoxazole nitrogen was within hydrogen bonding distance of the guanine 2-amino group of the G-tetrad, and (2) the amine of the dimethylamino tail would move slightly to associate proximal to a group peripheral to the intact G-tetrad, as seen in the case of **30**, with the phosphate in the sugar-phosphate TTA loop.

Thus, there is a specific structure-based reason for the expectation that the AIMs should be selective for G4 DNA at the expense of B. *The energy cost of B-DNA binding is increased by the mismatch with the helical pitch angle*.

3.2.5. Telomeric Repeat Amplification Protocol (TRAP) Assay—Stabilizing G-quadruplex inhibits telomerase activity, and this has been correlated with inhibition of cancer growth. Thus, until recently the TRAP assay has been widely used to assess G-quadruplex interaction. We reported in 2004 that the fluorescence analysis TRAPese assay was marred by the inhibition of *taq* polymerase by **32**,[52] and this recently has been verified by Mergny's group.[53] In the more reliable gel electrophoresis TRAP analysis, AIM **30** did indeed appear to inhibit telomere elongation rather than *taq* polymerase (data for both TRAPese and TRAP is shown in the Supplementary Material), however, we sought a more direct method of determining G4

interaction with our compounds, and therefore also examined electrospray mass spectrometry (*vide infra*).

3.2.6. Electrospray ionization mass spectrometry (ESI-MS) study of G-quadruplex DNA stabilization by 30 or 32—Total ions of G-quadruplex DNA, i-motif DNA, and duplex DNA were measured under the same conditions (Fig. 6.7). In the absence of G-4 stabilizing ligands (negative control), ion intensities of single-stranded DNA dropped dramatically, while duplex formation is rather fast. Rehvbridization in the absence of G4 stabilizing ligands proceeded to 50% completion in 10 minutes and was essentially complete in 45 minutes (negative control, shown in Supplementary Material). When incubated with either TMPyP4 (positive control), **30** or **32**, the decrease of single-stranded DNA signals and increase of duplex signals were dramatically slowed. Although no DNA-ligand complex ion was detected, the inhibition of duplex formation indicated interference from both TMPyP, **30**, and **32** in DNA annealing, which implies their ability for G-quadruplex stabilization. The slopes of ion intensity trend lines give approximate inhibition abilities of TMPyP4 and **32**. For example, slopes in total duplex ion intensity trends showed that TMPyP4 inhibited duplex formation at a comparable rate to **32**, where both took about 80 minutes to proceed to 50% hybridization, and significant ions corresponding to single stranded oligonuclotides were still present even at 2 hours.

4. Conclusion

The new compounds reported in this study showed *in vitro* antitumor activity, and the mean GI_{50} against the NCI60 cell line panel for the length of the oligopyrrole moiety (n= the number of pyrroles) was observed as $1 > 0 \gg 2 > 3$ for the bis-dimethylaminopropyl series **23**–**26)** and $1>2\gg0$ for the mono-dimethylaminopropyl series **(27–29)**; and for the anthracenyl C(10) position was $Ph\approx Cl \gg H > Br$ (**28**, **30–32**), with the most efficacious examples having average activity comparable to agents currently in general medical practice.[13] The activity correlates *inversely* with the length of lexitropsin oligopeptides within the conjugate molecules, that is, conjugates containing a *single pyrrole ring* demonstrated the strongest activity and broadest spectrum of inhibition against cancer cell lines. The SAR, spectroscopic and ES-MS assays are consistent with our current working hypothesis with the goal of selectively targeting G-4 sequences. In conclusion, the results presented suggest that the synthesis of a new series of anthracenyl isoxazole-lexitropsin conjugates, the AIMs, may represent a potential useful addition to the arsenal of anti-cancer molecules. In addition, we present structure–based evidence for the contention that the AIMs are unique among G4 binding agents in that they possess specific features which destabilize their intercalative interaction with B-DNA, and therefore, the expectation of selectivity is reasonable. Further clarification of the MoA and the effects of substitution at C5 of the isoxazole, and on the anthracene appears warranted. Those results will be reported in due course.

5. Experimental

Mass spectra were obtained on a JEOL JMS-AX505 HA. The NMR spectra (^{1}H and ^{13}C) were obtained on a Bruker AVANCE 300 and 500 Digital NMR (300 and 500 MHz, respectively) using SGI-IRIX 6.5. Elemental analysis was performed by Desert Analytics Laboratory, PO BOX 41838, Tucson, AZ 85717. All reactions were performed under an inert atmosphere of nitrogen or argon. Tetrahydrofuran was distilled from sodium-benzophenone immediately before use. Flash chromatography was performed on silica gel (Merck 60Å, 230–400mesh) with freshly distilled solvents. Pyrrole starting materials **2** and **3** were prepared according to Nishwaki.[21] 3-(9′-Anthracenyl) 5-methyl 4-isoxazolecaboxylate **17**, and the corresponding acridine **16**, [22] Anthracenyl ring analogs **18–20**[26].[27] and final product **33**[28] were prepared according to methodology previously reported by our lab.

2-[[[N,N-Bis[3-(N,N-dimethylamino)propyl]amino]carbonyl]-1-methyl-4-nitropyrrole(6)

To a solution of **3** (9.24 g, 35.88 mmol) in THF (40 mL), was added a solution of 3,3′-iminobis (N,N-dimethylpropylamine) (25.24 g, 134.74 mmol) at room temperature. The reaction mixture was heated at reflux for 3hrs. The reaction mixture was cooled to room temperature and the solvent was evaporated. The residue was then purified by chromatography on silica gel eluting with MeOH/Triethylamine (9/1) (Rf = 0.40) to give yellow oil **6** (4.82 g, 41.3%), which became a pale yellow solid after being triturated with hexane (20 mL); mp: 60–61 °C; ^{1}H NMR ($CDCl_3$): δ 7.69 (1H, d, J = 1.7 Hz), 7.66 (1H, d, J = 1.7 Hz), 3.96 (3H, s), 3.67 (4H, t, J = 7.5 Hz), 2.43-2.35 (16H, m), 1.94 (4H, m). ^{13}C NMR ($CDCl_3$): δ 162.4, 135.4, 127.2, 125.5, 106.7, 57.0, 46.0, 45.7, 37.0, 26.2. MS (CI): m/z (%) 340 (M+1, 100), 268 (8.62), 268 (8.62), 84 (12.83), 58 (18.52). Anal. Calcd. for $C_{16}H_{29}N_5O_3$: C, 56.62; H,8.61; N, 20.63. Found: C, 56.64; H, 8.33; N, 20.09.

2-[[[2-[[N,N-Bis[3-(N,N-dimethylamino)propyl]amino]carbonyl]-1-methyl-1H-pyrrol-4-yl] amino]carbonyl]-1-methyl-3-nitropyrrole (8)

To a solution of **6** (2.40 g, 7.38 mmol) in MeOH (175 mL), was added Pd/C (5%) (2.50 g). The mixture was hydrogenated at 37–40 psi at room temperature for 3hrs. The catalyst was removed by filtration and the solvent was removed *in vacuo*. To a solution of the above residue in THF (40 mL), was added a solution of **3** (3.05 g, 11.73 mmol) within 10 min. The reaction mixture was stirred at room temperature for 3 h. Solvent was removed *in vacuo* and the residue was then purified by chromatography on silica gel eluting with MeOH/Triethylamine (9/1) (Rf=0.34) to give pale yellow solid, 2.21 g (65%); mp: 125–127 °C. ^{1}H NMR ($CDCl_3$): δ 9.12 (1H, s), 7.61 (1H, d, J = 1.8Hz), 7.47 (1H, d, J = 1.8 Hz), 7.25 (1H, d, J = 1.8 Hz), 6.36 (1H, d, J = 1.8 Hz), 4.07 (3H, s), 3.71 (3H, s), 3.54 (4H, t, J = 7.8 Hz), 2.34 (4H, t, J = 7.2 Hz), 2.28 (12H, s), 1.85 (4H, m). ^{13}C NMR ($CDCl_3$): δ 164.1, 157.8, 135.2, 127.1, 126.8, 123.9, 121.3, 117.0, 107.8, 103.6, 57.1, 45.8, 45.6, 38.4, 36.1, 27.0; MS (CI): m/z (%) 462 (M+1, 100), 377 (19.91), 352 (14.52), 170 (67.70), 84 (28.51), 58 (17.97). To a solution of **8** (100 mg, 0.2 mmol) in absolute ethanol (5 mL), was added a solution of oxalic acid dihydrate ($C_2O_4H_2 \bullet 2H_2O$) (57 mg, 0.45 mmol). The mixture was stirred at room temperature until no more precipitate formed. The solid was filtered and washed with absolute ethanol (5 mL × 5). The oxalic acid salt of **8** was obtained after being dried *in vacuo* to yield a solid (109 mg, 90%), mp: 203–204 °C. Anal. Calcd. for $C_{22}H_{35}N_7O_4 \bullet 1.5C_2O_4H_2 \bullet 0.5H_2O$ (%): C, 49.58; H, 6.49; 16.19. Found: C, 49.81; H, 6.64; N, 16.05.

2-[[[2-[[[2-[[N,N-Bis[3-(N,N-dimethylamino)propyl]amino]carbonyl]-1-methyl-1H-pyrrol-4-yl]amino]carbonyl]-1-methyl-1H-pyrrol-4-yl]amino]carbonyl]-1-methyl-4-nitropyrrole (10). To a solution of 8 (1.13 g, 2.45 mmol) in MeOH (90 mL), was added Pd/C (5%) (2.00 g). The mixture was hydrogenated at 37–40 psi at room temperature for 3 h. The catalyst was removed by filtration and the solvent was removed *in vacuo*. To a solution of the above residue in THF (30 mL), was added a solution of 3 (1.00 g, 3.90 mmol) within 10 min. The reaction mixture was stirred at room temperature of 3 h. Solvent was removed in vacuo and the residue was then purified by chromatography on silica gel eluting with MeOH/ Triethylamine (9/1) (Rf = 0.21) to give pale yellow solid, (0.74 g, 52%); mp: 178–179 °C; ^{1}H NMR (DMSO-d_6): δ 10.29 (1H, s), 9.89 (1H, s), 8.18 (1H, d, J = 1.7 Hz), 7.58 (1H, d, J = 1.7 Hz), 7.24 (2H, d, J = 1.7 Hz), 7.03 (1H, d, J = 1.7 Hz), 6.37 (1H, d, J = 1.7 Hz); 3.96 (3H, s), 3.85 (3H, s), 3.58 (3H, s), 2.49 (4H, t, J = 7.7 Hz), 2.15 (4H, t, J = 7.1 Hz), 2.10 (12H, s), 1.70-1.61 (4H, m). ^{13}C NMR ($CDCl_3$): δ 164.6, 159.2, 158.1, 135.4, 127.3, 126.7, 124.0, 123.6, 123.0, 121.8, 120.0, 117.6, 108.5, 102.9, 102.6, 57.1, 46.4, 45.6, 38.7, 37.2, 35.9, 27.1. MS (CI): m/z (%) 584 (M+1, 55.96), 397 (10.47), 275 (24.39), 153 (18.31), 149 (52.19), 122 (32.51), 107 (20.18), 101 (16.14), 81 (100). Anal. Calcd. for $C_{28}H_{41}N_9O_5$ (%): C, 57.62; H, 7.08; N, 21.60. Found: C, 57.23; H, 7.26; N, 21.24.

Ethyl 3-(10′-phenyl-9′-anthracenyl)-5-methyl-4-isoxazole carboxylate (20)

A mixture of ethyl 3-(10′-bromo-9′-anthracenyl)-5-methyl-4-isoxazole carboxalate (420 mg, 1.02 mmol), phenyl boronic acid (140 mg, 1.15 mmol), $Pd_2(dba)_3$ (45 mg, 5 mol%), P(t-Bu)$_3$ (10% in hexane, 242 mg, 12 mol%) and KF (191 mg, 3.3 mmol) in THF (7 mL)was stirred at room temperature under argon atmosphere for 72 h. The reaction mixture was filtered and the solid was washed by THF (10 mL). The filtrate was concentrated and purified by chromatography on silica gel eluting with hexane/benzene (3:2) to give yellow crystal (382 mg, 92%); mp: 178–180 °C. ^{1}H NMR ($CDCl_3$): δ 7.62 (4H, m), 7.52 (3H, m), 7.32 (6H, m), 3.68 (2H, q, J = 7.2 Hz), 2.88 (3H, s), 0.33 (3H, t, J = 7.2 Hz). ^{13}C NMR ($CDCl_3$): δ 176.2, 161.5, 160.8, 139.3, 138.6, 131.2, 131.1, 130.5, 129.7, 129.0, 128.5, 128.4, 128.3, 127.6, 127.1, 125.9, 125.5, 125.1, 122.8, 111.5, 60.1, 13.5, 12.8. MS (EI): m/z (%) 407 (M^+, 100), 319 (17.91), 295 (12.85), 252 (13.86). Anal. Calcd for $C_{27}H_{21}NO_3$: C, 79.59; H, 5.19; N, 3.44. Found: C, 79.94; H, 5.09; N, 3.57.

3-(9-Anthracenyl)- N,N-bis[3-(N,N-dimethylamino)propyl]-5-methyl-4-isoxazole carboxamide (23)

To a suspension of anhydrous $SmCl_3$ (0.21 g, 0.79 mmol) in THF (6 mL) was added ethyl 3-(9-anthracenyl)-5-methyl-4-isoxazolecarboxylate **17** (0.25 g, 0.72 mmol) in dry THF (5 mL). The mixture was stirred under nitrogen at room temperature for 5.5 h and was ready to be used in the following steps.

In a solution of 3,3′-iminobis(N,N-dimethylpropylamine) (0.222 g, 1.19 mmol) in THF (10 mL) was added $(CH_3)_3Al$ (2M in hexane, 0.75 mL) at 0 °C during 30 min. The mixture turned into yellow. Warmed up the reaction to room temperature and kept the reaction going for another 1 h, until it was ready to be transferred in next step.

To the above-prepared mixture containing activated ester, was added the brown solution of the above prepared activated amino-lexitropsin solution at room temperature during 10 min. Kept the final mixture refluxing for 8 h. Na_2SO_4●$10H_2O$ (1.0 g) and cold methanol (20 mL) were added to the reaction mixture in order to quench the excessive $(CH_3)_3Al$. Solid was removed through centrifuge and a red solution was collected. The red solution was concentrated and purified by chromatography on silica gel (200–400mesh) eluting with methanol/30% NH_4OH (95:5), to afford yellow oil (0.32 g, 87%). ^{1}H NMR ($CDCl_3$): δ 8.58 (1H, s), 8.06-8.00 (4H, m), 7.54-7.47 (4H, m), 3.06 (2H, t, J = 7.1 Hz), 2.74 (3H, s), 2.53 (2H, t, J = 7.1 Hz), 2.00 (6H, s), 1.87 (6H, s), 1.63 (2H, t, J = 6.9 Hz), 1.45 (2H, t, J = 6.9 Hz), 1.11-0.95 (2H, m), 0.90-0.83 (2H, m). ^{13}C NMR ($CDCl_3$): δ 170.8, 163.1, 157.8, 131.4, 131.1, 130.8, 130.3, 129.7, 129.3, 128.8, 128.7, 128.3, 127.1, 126.2, 125.8, 125.3, 121.9, 116.3, 56.2, 47.4, 46.4, 45.6, 45.4, 42.5, 26.7, 24.9, 11.5; MS (CI): m/z (%) 473 (M+1, 100), 188 (22.58), 58 (18.63). To a solution of **23** (94 mg, 0.2 mmol) in absolute ethanol (5 mL), was added a solution of oxalic acid dihydrate ($C_2O_4H_2$ ●$2H_2O$) (57 mg, 0.45 mmol). The mixture was stirred at room temperature until no more precipitate formed. The solid was filtered and washed with absolute ethanol (5 mL × 5). The oxalic acid salt of **23** was obtained after being dried *in vacuo* to yield a solid (114mg, 84%), mp: 185–186°C. Anal. Calc'd. for $C_{29}H_{36}N_4O_2$●$2C_2H_2O_4$●$1.5H_2O$: C, 58.31; H, 6.38; N,●8.24. Found: C, 58.50; H, 6.12; N, 8.12.

3-(9-Anthracenyl)-N-[2-[[N,N-Bis[3-(N,N-dimethylamino)propyl] amino] carbonyl]-1-methyl-1H-pyrrol-4-yl]-5-methyl-4-isoxazolecarboxamide (24)

To a suspension of anhydrous $SmCl_3$ (0.21 g, 0.79 mmol) in THF (10 mL) was added **17** (0.25 g, 0.72 mmol) in dry THF (10 mL). The mixture was stirred under nitrogen at room temperature for 5.5 hrs and was ready to be used in the following steps.

A suspension of 10 % Pd/C (0.2 g) in a solution of **6** (0.385 g, 1.19 mmol) in methanol (30 mL), was stirred for 4.5 h under H_2 pressure (37 psi) at room temperature. The catalyst was removed by filtration, and the solvents removed *in vacuo*. The hydrogenation product was dissolved into dry THF (15 mL) and $(CH_3)_3Al$ (2M in hexane, 0.75 mL) was added at 0 °C during 30 min. The mixture turned into brown. Warmed up the reaction to room temperature and kept the reaction going for another 1 hr., until it was ready to be transferred in next step.

To the above-prepared mixture containing activated ester, was added the brown solution of the above prepared activated amino-lexitropsin solution at room temperature during 10 min. The mixture was refluxed for 8 h. $Na_2SO_4\bullet 10H_2O$ (1.0 g) and cold methanol (20 mL) were added to the reaction mixture in order to quench the excessive $(CH_3)_3Al$. Solid was removed through centrifuge and a red solution was collected. The red solution was concentrated and chromatography was performed on silica gel (200–400mesh), using methanol/30% NH_4OH (95:5), to afford a pale yellow solid (0.396 g 84%), mp: 109–111°C. ^1H NMR ($CDCl_3$): δ 8.63 (1H, s), 8.04(2H, dd, J = 0.9, 8.3 Hz), 7.65 (2H, dd, J = 0.9, 8.3 Hz), 7.52-7.23 (4H, m), 6.56 (1H, d, J = 1.7 Hz), 6.40 (1H, s), 4.90 (1H, d, J = 1.7 Hz), 3.37 (3H, s), 3.21 (4H, t, J = 6.6 Hz), 2.94 (3H, s), 2.24-1.90 (16H, m), 1.60-1.45 (4H, m), 1.52 (2H, s). ^{13}C NMR ($CDCl_3$): δ 176.3, 163.9, 158.0, 157.9, 157.8, 157.6, 131.5, 131.2, 130.7, 129.2, 128.9, 128.4, 128.2, 127.9, 126.5, 125.8, 125.7, 125.3, 124.3, 120.7, 120.3, 116.1, 113.2, 57.2, 46.4, 45.8, 35.6, 26.6, 14.0. MS (CI): m/z (%) 595 (M+1, 100), 510 (6.09), 336 (19.88). Anal. Calc'd for $C_{35}H_{42}N_6O_3\bullet H_2O$: C, 68.60; H, 7.24; N, 13.71. Found: C, 68.33; H, 6.94; N, 13.61.

3-(9-Anthracenyl)-N-[2-[[[2-[[N,N-Bis[3-(N,N-dimethylamino)propyl]amino]carbonyl]-1-methyl-1H-pyrrol-4-yl]amino]carbonyl]-1-methyl-1H-pyrrol-4-yl]-5-methyl-4-isoxazolecarboxamide (25)

By the same procedure as that described for **24**, from $SmCl_3$ (0.21 g, 0.79 mmol), **17** (0.25 g, 0.72 mmol), 10 % Pd/C (0.2 g), **8** (0.55 g, 1.19 mmol) and $(CH_3)_3Al$ (2M in hexane, 0.75 mL), **25** was obtained as a pale yellow solid (0.44 g 78%); mp: 118–120°C (dec). ^1H NMR ($CDCl_3$): δ 8.72 (1H, s), 8.12 (2H, dd, J = 0.9, 8.2 Hz), 7.70 (2H, dd, J = 0.9, 8.2 Hz), 7.55-7.50 (4H, m), 7.19 (1H, s), 7.09 (1H, d, J = 1.7 Hz), 6.41 (1H, s), 6.28 (1H, d, J = 1.7Hz), 6.10 (1H, d, J = 1.7 Hz), 5.69 (1H, d, J = 1.7 Hz), 3.65 (3H, s), 3.61 (3H, s), 3.48 (4H, t, J = 7.8 Hz), 2.99 (3H, s), 2.28-2.10 (16H, m), 1.83-1.69 (4H, m), 1.52 (5H, s). ^{13}C NMR ($CDCl_3$): δ 176.7, 164.3, 158.7, 158.5, 157.8, 131.5, 131.3, 130.9, 129.3, 129.0, 128.6, 128.4, 128.0, 126.6, 125.9, 125.7, 125.3, 124.3, 123.6, 121.2, 120.6, 120.5, 118.8, 116.7, 113.0, 103.3, 103.2, 103.0, 57.3, 46.4, 45.7, 36.9, 35.9, 26.8, 14.1. MS (FAB): m/z (%) 717 (M+1, 71), 530, (13.19), 286 (15.85), 230 (12.43), 271 (12.37), 244 (59.35), 214 (20.21), 188 (12.72), 149 (61.28), 122 (49.88), 106 (16.22), 81 (100). Anal. Calc'd for $C_{41}H_{48}N_8O_4\bullet 2.5H_2O$: C, 64.63; H, 7.01; N, 14.71. Found: C, 64.77; H, 6.64; N, 15.08.

3-(9-Anthracenyl)-N-[2-[[[2-[[[2-[[N,N-Bis[3-(N,N-dimethylamino)propyl]amino] carbonyl]-1-methyl-1H-pyrrol-4-yl]amino]carbonyl]-1-methyl-1H-pyrrol-4-yl]amino] carbonyl]-1-methyl-1H-pyrrol-4-yl]]-5-methyl-4-isoxazolecarboxamide (26)

By the same procedure as that described for **24**, from $SmCl_3$ (0.21 g, 0.79 mmol), 17 (0.25 g, 0.72 mmol), 10 % Pd-C (0.2 g), **10** (0.693g, 1.19 mmol) and $(CH_3)_3Al$ (2M in hexane, 0.75 mL), **26** was obtained as a pale yellow solid (0.37g, 56%), mp: 131–133 °C (dec). ^1H NMR ($CDCl_3$): δ 8.56 (1H, s), 7.96 (2H, dd, J = 0.8, 8.1 Hz), 7.62 (2H, dd, J = 0.8, 8.1 Hz), 7.46-7.30 (4H, m), 7.08 (1H, d, J = 1.8Hz), 6.98 (1H, s), 6.89 (1H, d, J=1.8Hz), 6.59 (1H, s), 6.38 (1H, d, J = 1.8Hz), 6.28 (1H, d, J = 1.8 Hz), 6.23 (1H, d, J=1.8Hz), 6.20 (1H, d, J = 1.8 Hz), 5.78 (1H, s), 3.83 (3H, s), 3.58 (3H, s), 3.54 (3H, s), 3.44 (4H, t, J = 7.2 Hz), 2.91 (3H, s), 2.16-2.10 (16H, m), 1.72-1.65 (4H, m), 1.53(3H, s) ^{13}C NMR ($CDCl_3$): δ 179.6, 176.6, 176.0, 175.6, 170.8, 169.8, 159.6, 159.3, 158.5, 158.0, 131.4, 130.7, 129.1, 128.2, 128.1, 127.7, 126.3, 125.5, 124.9, 123.7, 123.5, 122.2, 121.9, 120.5, 120.1, 119.4, 118.9, 117.0113.3, 104.3, 103.9, 103.4,

57.0, 46.1, 45.4, 36.8, 36.7, 35.6, 13.8. MS (FAB): m/z (%) 839 (M+1, 43), 717 (11.64), 286 (29.71), 277 (15.81), 271 (25.40), 244 (100), 214 (31.05), 149 (87.91), 123 (64.75), 85 (86.34). Anal. Calc'd for $C_{47}H_{54}N_{10}O_5 \bullet 1.5H_2O$) C, 65.18; H, 6.63; N, 16.17. Found: C, 65.37; H, 6.56; N, 15.83.

3-(10′-Chloro-9′-anthracenyl)-N-[2-[[N-[3-(N,N-dimethylamino)-propyl]amino]carbonyl]-1-methylpyrrol-4-yl]-5-methyl-4-isoxazolecarboxamide (30)

To a suspension of anhydrous $SmCl_3$ (393.5 g, 1.53 mmol) in THF (10 mL) was added **18** (381.3 mg, 1.04 mmol) in dry THF (10 mL). The mixture was stirred under nitrogen at room temperature for 5.5 h and was ready to be used in the following steps.

A suspension of 10 % Pd/C (310.6mg) in a solution of **12** (473.0 g, 1.86 mmol) in methanol (30 mL), was stirred for 4.5 h under H_2 pressure (37 psi) at room temperature. The catalyst was removed by filtration, and the solvents were removed *in vacuo*. The hydrogenation product was dissolved into dry THF (15 mL) and $(CH_3)_3Al$ (2M in hexane, 2 mL) was added at 0 °C during 30 min. The mixture turned into brown. Warmed up the reaction to room temperature and kept the reaction going for another 1 h, until it was ready to be transferred in next step. To the above-prepared mixture containing activated ester, was added the brown solution of the above prepared activated amino-lexitropsin solution at room temperature during 10 min. The final mixture was refluxed for 18 h. $Na_2SO_4 \bullet 10H_2O$ (1.0 g) and cold methanol (20 mL) were added to the reaction mixture in order to quench the excessive $(CH_3)_3Al$. Solid was removed through centrifuge and a red solution was collected. The red solution was concentrated and purified by chromatography on silica gel (200–400mesh) eluting with methanol/30% NH_4OH (95:5), to afford a pale yellow solid (203.7 mg, 36%), mp: 208–210 °C. ^1H NMR ($CDCl_3$): δ 8.65 (2H, dt, J = 5.4, 0.6 Hz), 7.78 (1H, br), 7.73 (2H, dt, J = 5.4, 0.6 Hz), 7.69 (2H, m), 7.57 (2H, m), 6.76 (1H, d, J = 1.2 Hz), 6.40 (1H, s), 5.19(1H, d, J = 1.2 Hz), 3.72 (3H, s), 3.31 (2H, q, J = 3.6 Hz), 3.02 (3H, s), 2.36 (2H, t, J = 3.6 Hz), 2.08 (3H, s), 1.58 (2H, m). ^{13}C NMR ($CDCl_3$): δ 176.5, 161.1, 157.7, 157.0, 132.8, 131.3, 128.5, 128.1, 127.6, 125.5, 125.4, 123.8, 120.2, 119.8, 118.3, 112.9, 101.5, 59.4, 45.4, 39.9, 36.5, 25.1, 13.8. MS (CI): m/z (%) 544.00 (M^+, 65.88), 306.90 (58.70), 288.92 (24.86), 153.96 (100), 136.99 (90.87). Anal. Cal'd. for $C_{30}H_{30}ClN_5O_3$: C, 66.23; H, 5.56; N, 12. 87. Found: C, 66.07; H, 5.50; N, 12.71.

3-(10′-Br-9′-anthracenyl)-N-[2-[[N-[3-(N,N-dimethylamino)-propyl]amino]carbonyl]-1-methylpyrrol-4-yl]-5-methyl-4-isoxazolecarboxamide (31)

By the same procedure as that described for **30**, from $SmCl_3$ (481.5 mg, 1.87 mmol), **19** (341.6 mg, 0.83 mmol), 10 % Pd/C (490 mg), **12** (458.5 mg, 1.80 mmol) and $(CH_3)_3Al$ (2M in hexane, 2 mL), **31** was obtained as a yellow solid (280mg, 61%), mp: 201.5–203.5 °C. ^1H NMR ($CDCl_3$): δ 8.70 (2H, d, J = 9 Hz), 7.71 (5H, m), 7.60 (2H, m), 7.57 (2H, m), 6.74 (1H, d, J = 1.5 Hz), 6.40 (1H, s, br), 5.24 (1H, d, J = 1.5 Hz), 3.74 (3H, s), 3.32 (2H, q, J = 3.6 Hz), 3.04 (3H, s), 2.38 (2H, t, J = 3.6 Hz), 2.11 (6H, s), 1.61 (2H, m). ^{13}C NMR ($CDCl_3$): δ 176.4, 161.0, 157.7, 157.0, 131.4, 130.3, 128.4, 128.0, 127.9, 127.0, 125.4, 123.8, 121.3, 119.7, 118.2, 112.9, 101.6, 59.3, 45.4, 39.7, 36.4, 25.2, 13.6. MS (CI): m/z (%) 590.01 (M+1, 100.00), 588.02 (99.87), 542.97 (19.06), 485.88 (22.84), 321.85 (31.82), 242.96 (20.71), 153.99 (50.75), 136.00 (51.68), 129.09 (65.34), 84.38 (43.93). Anal. Calc'd. for $C_{30}H_{30}BrN_5O_3$: C, 61.23; H, 5.14; N, 11.90. Found: C, 61.16; H, 5.29; N, 11.62.

3-(10′-phenyl-9′-anthracenyl)-N-[2-[[N-[3-(N,N-dimethylamino)-propyl]amino]carbonyl]-1-methylpyrrol-4-yl]-5-methyl-4-isoxazolecarboxamide (32)

By the same procedure as that described for **30**, from $SmCl_3$ (491.5 mg, 1.90 mmol), **19** (300.6 mg, 0.73 mmol), 10 % Pd/C (553 mg), **12** (500.5 mg, 1.97 mmol) and $(CH_3)_3Al$ (2M in hexane, 2 mL), **32** was obtained as a pale yellow solid, 130 mg (30%), mp: 126–128°C. ^1H NMR ($CDCl_3$): δ 7.68 (3H, m), 7.45 (10H, m), 6.49 (1H, s), 6.47 (1H, s), 5.37(1H, s), 3.65 (3H, s),

3.25 (2H, q, 3.6Hz), 2.96 (3H, s), 2.27 (2H, t, J=3.6Hz), 2.01 (6H, s), 1.53 (2H, m). ^{13}C NMR ($CDCl_3$): δ 176.2, 161.5, 160.1, 157.3, 139.4, 138.8, 131.4, 131.1, 130.5, 129.7, 129.0, 128.5, 128.4, 128.3, 127.6, 127.1, 125.9, 125.5, 125.1, 123.8, 122.8, 119.8, 118.1, 111.5, 101.7, 60.1, 45.4, 39.6, 36.1, 25.0, 13.4. MS (EI): m/z (%) 587 (M+1, 39.04), 586 (M^+, 100), 585 (M−1, 19.26), 484 (13.13), 320 (19.84). Anal. Calc'd. for $C_{36}H_{35}N_5O_3$:C, 73.82; H, 6.02; N, 11.96. Found: C, 68.39; H, 5.85; N, 11.60.

In vitro anti-tumor assays—The NCI's in vitro anti-tumor screen(Alley, Scudiero et al. 1988; Boyd 1989; Boyd and Paull 1995)13, 36, 37 consists of 60 human tumor cell lines against which compounds 22–33 are tested at a minimum of five concentrations at 10-fold dilutions. A 48 h continuous drug exposure protocol is used, and a sulforhodamine B (SRB) protein assay is used to estimate cell viability or growth.

Acknowledgments

NRN thanks the National Institute of Neurological Disease and Stroke for Grant NS38444 and P20RR015583. We would like to thank the University of Idaho Research Council, and the National Cancer Institute for financial support. Dr. Dan Zaharevitz assisted us with the COMPARE calculation and interpretation. XH, CL and KCR, acknowledge the Malcolm and Carol Renfrew Scholarship Endowment, University of Idaho. CL and KCR also thank P20RR16454.

References

1. Hurley LH. DNA and associated targets for drug design. J Med Chem 1989;32:2027–2033. [PubMed: 2671370]
2. Damia G, Broggini M. Improving the selectivity of cancer treatments by interfering with cell response pathways. Eur J Cancer 2004;40:2550–2559. [PubMed: 15541958]
3. Di Marco A. Mechanism of action and mechanism of resistance to antineoplastic agents that bind DNA. Antibiotics and Chemotherapy 1978;23:216–227. [PubMed: 348080]
4. Dervan PB. Design of sequence-specific DNA-binding molecules. Science 1986;232:464–471. [PubMed: 2421408]
5. Dervan PB. Molecular recognition of DNA by small molecules. Bioorg Med Chem 2001;9:2215–2235. [PubMed: 11553460]
6. Bailly C, Chaires JB. Sequence specific DNA minor groove binders: Design and synthesis of netropsin and distamycin analogues. Bioconjugate Chem 1998;9:513–538.
7. Cech TR. G-strings at chromosome ends. Nature 1988;332:777–778. [PubMed: 3357543]
8. Zahler AM, Williamson JR, Cech TR, Prescott DM. Inhibition of telomerase by G-quartet structures. Nature 1991;350:718–720. [PubMed: 2023635]
9. Cech TR. Life at the end of the chromosome: Telomeres and telomerase. Angew Chem 2000;39:34–43. [PubMed: 10649348]
10. Phan AT, Mergny J-L. Human telomeric DNA: G-quadruplex, i-motif and Watson-Crick double helix. Nucleic Acids Res 2002;30:4618–4625. [PubMed: 12409451]
11. Verner EJ, Oliver BJ, Schlicksupp L, Natale NR. The use of phosphonitrilic dichloride cyclic trimer in oligopeptide synthesis: Synthesis of isoxazolyl-prodrugs of netropsin and distamycin. Heterocycles 1990;31:327–339.
12. Zhou P, Mosher MD, Taylor WD, Crawford GA, Natale NR. Double activation preparation of an acridinyl-isoxazolyl-lexitropsin. Bioorg Med Chem Lett 1997;7:2455–2456.
13. Boyd MR. Status of the NCI preclinical antitumor drug discovery screen. Principles & Practices of Oncology 1989;3:1–12.
14. Sausville, EA.; Johnson, JI.; Cragg, GM.; Decker, S. Cancer drug discovery and development: New paradigms for a new millennium. In: Ojima, I.; Vite, GD.; Altmann, K., editors. Anticancer Agents, Frontiers in Cancer Chemotherapy. ACS Symposium Series 796, ACS; Washington D.C.: 2001. p. 1-15.
15. Han H, Hurley LH. G-quadruplex DNA: A potential target for anticancer drug design. Trends Pharmacol Sci 2000;21:136–142. [PubMed: 10740289]

16. Hurley LH, Wheelhouse RT, Sun D, Kerwin SM, Salazar M, Ferdoroff OY, Han FX, Han H, Zbicka E, Von Hoff DD. G-quadruplexes as targets for drug design. Pharmacol Ther 2000;85:141–158. [PubMed: 10739869]
17. Neidle S. Targeting the end of DNA. Chem Br 2000;36:27–29.
18. Neidle S, Kelland LR. Commentary. Telomerase as an anti-cancer target: Current status and future prospects. Anti-Cancer Drug Des 1999;14:341–347.
19. Siddiqui-Jain A, Grand CL, Bearss DJ, Hurley LH. Direct evidence for a G-quadruplex in a promoter region and its targeting with a small molecule to repress c-MYC transcription. Proc Natl Acad Sci USA 2002;99:11593–11598. [PubMed: 12195017]
20. Gendler PL, Rapoport H. Permethyl analogue of the pyrrolic antibiotic distamycin A. J Med Chem 1981;24:33–38. [PubMed: 7009865]
21. Nishiwaki E, Tanaka S, Lee H, Shibuya M. Efficient synthesis of oligo-N-methylpyrrolecarboxamides and related compounds. Heterocycles 1988;27:1945–1952.
22. Mosher MD, Natale NR. The Preparation of Intercalating Isoxazoles via a Nitrile Oxide Cycloaddition. J Hetereocycl Chem 1995;32:779–781.
23. Basha A, Lipton M, Weinreb SM. A mild, general method for conversion of esters to amides. Tetrahedron Lett 1977:4171–4174.
24. Mosher MD, Natale NR, Vij A. An intercalating isoxazole. Acta Crystallogr, Sect C 1996;C52:2513–2515.
25. Shen ZQ, Wang FS, Hu ZY, Yu FS, Qian BG. The characteristics of lanthanide coordination catalysts and the polydienes prepared therewith. J Polym Sci, Polym Chem Ed 1980;18:3345–3357.
26. Han X, Li C, Rider KC, Blumenfeld A, Twamley B, Natale NR. The Isoxazole as a linchpin for molecules which target folded DNA conformations: Selective Lateral Lithiation and Palladation. Tetrahedron Lett 2002;43:7673–7677.
27. Han X, Twamley B, Natale NR. Preparation of 3-(10′-Halo-9′-anthracenyl)-5-methyl isoxazolecarboxylic Esters. J Heterocycl Chem 2003;40:539–545.
28. Han X, Natale NR. Design and Synthesis of a Novel Intercalating Bis-lexitropsin Conjugate. J Heterocycl Chem 2001;38:415–418.
29. Eliadis A, Phillips DR, Reiss JA, Skorobogaty A. The synthesis and DNA footprinting of acridine-linked netropsin and distamycin bifunctional mixed ligands. J Chem Soc, Chem Commun 1988:1049–1052.
30. Bai RL, Paull KD, Herald CL, Malspeis L, Pettit GR, Hamel E. Halichondrin B and homohalichondrin B, marine natural products binding in the vinca domain of tubulin: Discovery of tubulin-based mechanism of action by analysis of differential cytotoxicity data. J Biol Chem 1991;266:15882–15889. [PubMed: 1874739]
31. Paull KD, Lin CM, Malspeis L, Hamel E. Identification of novel antimitotic agents acting at the tubulin level by computer-assisted evaluation of differential cytotoxicity data. Cancer Res 1992;52:3892–3900. [PubMed: 1617665]
32. Mergny JL, Helene C. G-quadruplex DNA: A target for drug design. Nature medicine 1998;4:1366–1367.
33. Mergny JL, Mailliet P, Lavelle F, Riou JF, Laoui A. The development of telomerase inhibitors: The G-quartet approach. Anti-Cancer Drug Des 1999;14:327–339.
34. Kerwin SM. G-quadruplex DNA as a target for drug design. Curr Pharm Des 2000;6:441–478. [PubMed: 10788591]
35. Cuesta J, Read MA, Neidle S. The design of G-quadruplex ligands as telomerase inhibitors. Mini Reviews in Medicinal Chemistry 2003;3:11–21. [PubMed: 12570851]
36. Youngquist RS, Dervan PB. Sequence-specific recognition of B-DNA by oligo(N-methylpyrrolecarboxamide)s. Proc Natl Acad Sci USA 1985;82:2565–2569. [PubMed: 2986122]
37. White S, Baird EE, Dervan PB. On the pairing rules for recognition in the minor groove of DNA by pyrrole-imidazole polyamides. Chemi Biol 1997;4:569–578.
38. Wakefield BJ, Wright DJ. Isoxazole chemistry since 1963. Adv Heterocycl Chem 1979;25:147–204.

39. Alley MC, Scudiero DA, Monks A, Hursey ML, Czerwinski MJ. Feasibility of drug screening with panels of human tumor cell lines using a microculture tetrazolium assay. Cancer Res 1988;48:589–601. [PubMed: 3335022]
40. Boyd MR, Paull KD. Some practical considerations and applications of the National Cancer Institute in vitro anticancer drug discovery screen. Drug Dev Res 1995;34:91–109.
41. Han FX, Wheelhouse RT, Hurley LH. Interactions of TMPyP4 and TMPyP2 with Quadruplex DNA. Structural Basis for the Differential Effects on Telomerase Inhibition. J Am Chem Soc 1999;121:3561–3570.
42. [Last accessed on Oct. 14, 2008]. http://dtp.nci.nih.gov/docs/compare/compare_intro.html
43. Boyd, MR.; Paull, KD.; Rubinstein, LR. Cytotoxic Anticancer Drugs: Models and Concepts for Drug Discovery and Development. Vleriote, FA.; Corbett, TH.; Baker, LH., editors. Kluwer Academic; Hingham, MA: 1992. p. 11-34.
44. Li C, Twamley B, Natale NR. Ethyl 3-(10-chloroanthracenyl)-5-(1-phenyl-2-hydroxylethylenyl) isoxazole-4-carboxylate: an enol from Dess-Martin oxidation. Acta Cryst E 2006;E62:o854–o856.
45. Li C, Twamley B, Natale NR. Preparation and Crystal Structures of Two 3-Anthracenyl Isoxazolyl Sulfonamides. J Heterocycl Chem. 2008 in press.
46. Goodsell D, Dickerson RE. Isohelical analysis of DNA groove-binding drugs. J Med Chem 1986;29:727–733. [PubMed: 2422377]
47. Goodsell DS, Ng HLKopka ML, Lown JW, Dickerson RE. Structure of a dicationic monoimidazole lexitropsin bound to DNA. Biochemistry 1995;34:16654–16661. [PubMed: 8527438]
48. Zamponi G, Stotz SC, Staples RJ, Rogers TA, Nelson JK, Hulubei V, Blumenfeld A, Natale NR. Unique Structure Activity Relationship of 4-Isoxazolyl-1,4-dihydropyridines. J Med Chem 2003;46:87–96. [PubMed: 12502362]
49. Mehta AK, Shayo Y, Vankayalapati H, Hurley LH, Schaefer J. Biochemistry 2004;43:11953. [PubMed: 15379535]
50. Parkinson GN, Lee MP, Neidle S. Crystal structure of parallel quadruplexes from human telomeric DNA. Nature 2002;417:876–880. [PubMed: 12050675]
51. Clark GR, Pytel PD, Squire CJ, Neidle S. Structure of the first parallel DNA quadruplex-drug complex. J Am Chem Soc 2003;125:4066–4067. [PubMed: 12670225]
52. Li, C.; Rider, K.; Fusco, W.; Natale, NR.; Crawford, R. Synthesis and Activity of Anti-cancer Compounds that Target G-quadruplex DNA. 227th ACS National Meeting; Anaheim, CA. March 28-April 1, 2004; MEDI 142. See also Chemical & Engineering News. March 8;2004 TECH-76.
53. DeCian A, Cristofari G, Reichenbach P, De Lemos E, Monchaud D, Teulade-Fichou M, Shin-ya K, Lacroix L, Lingner J, Megny J. PNAS 2007;104:17347–17352. [PubMed: 17954919]
54. Wozczk M, Grzesiak E, Kowalczyk D, Ostaszewski R. Interactions of New Derivatives of Anthracene with Calf Thymus DNA. Proc SPIE 2002;4749:259–266.
55. Kumar CV, Asuncion EH. DNA Binding Studies and Site Selective Fluorescence Sensitization of an Anthryl Probe. J Am Chem Soc 1993;115:8541–8553.
56. Samudrala R, Zhang XM, Wadkins RM, Mattern DL. Synthesis of a Non-cationic, Water-soluble Perylenetetracarboxylic Diimide and Its Interactions with G-quadruplex-forming DNA. Bioorganic & Medicinal Chemistry 2007;15:186–193. [PubMed: 17079147]
57. Zhuang X, Tang J, Hao Y, Tan Z. Fast Detection of Quadruplex Structure in DNA by The Intrinsic Fluorescence of a Single-stranded DNA Binding protein. J Mol Recognit 2007;20:386–391. [PubMed: 17891754]
58. (a) Hollingshead MG, Alley MC, Camalier RF, Abbott BJ, Mayo JG, Malspeis L, Grever MR. Life Sci 1995;57:131. [PubMed: 7603295] (b) Bollini M, Casal JJ, Bruno AM. Bioorg Med Chem 2008;16:8003–8010. [PubMed: 18715786]
59. (a) Mitani S, Kamata H, Fujiwara M, Aoki N, Tango T, Fukuchi K, Oka T. Analysis of c - myc DNA amplification in non - small cell lung carcinoma in comparison with small cell lung carcinoma using polymerase chain reaction. Clinical and Experimental Medicine 2001;1(2):105–111. [PubMed: 11699727] (b) Broers, Jos LV.; Viallet, Jean; Jensen, Sandra M.; Pass, Harvey; Travis, William D.; Minna, John D.; Linnoila, RIlona. Expression of c - myc in progenitor cells of the bronchopulmonary epithelium and in a large number of non - small cell lung cancers. American Journal of Respiratory Cell and Molecular Biology 1993;9(1):33–43. [PubMed: 8393325] (c) Arango D, Mariadason JM,

Wilson AJ, Yang W, Corner GA, Nicholas C, Aranes MJ, Augenlicht LH. c-Myc overexpression sensitises colon cancer cells to camptothecin-induced apoptosis. British Journal of Cancer 2003;89 (9):1757–1765. [PubMed: 14583781] (d) Simonsson T, Pecinka P, Kubista M. DNA Tetraplex Formation in The Control Region of c-myc. Nucleic Acids Res 1998;26:1167–1172. [PubMed: 9469822]

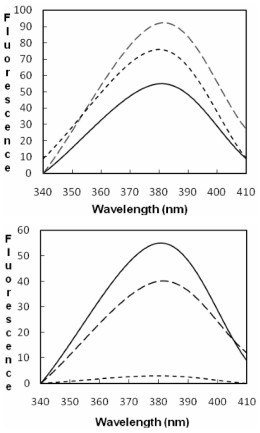

Figure 1.

Figure 1a. Normalized Fluorescence spectra of AIM-**29** alone (solid line), CT-DNA alone (long-dashed line) and the Hurley Oligonucleotide alone (small-dashed line).

Figure 1b. Normalized Fluorescence spectra of AIM-**29** alone (solid line), with CT-DNA (long-dashed line) and the Hurley-sequence Oligonucleotide (small-dashed line).

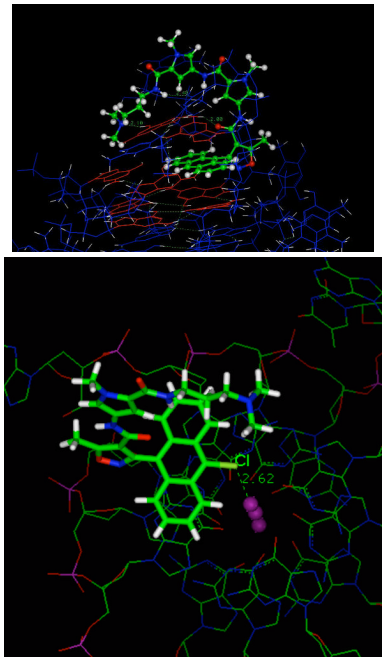

Figure 2.
Plausible Docking modes of compounds **29** and **30.** (a) Top, the Intercalative mode, where **29** is shown displacing a guanine after minimization (b) Bottom, the stacking mode with ligand **30**, after minimization the Chlorine nestles within a reasonable association distance with the potassium in the G-tetrad.

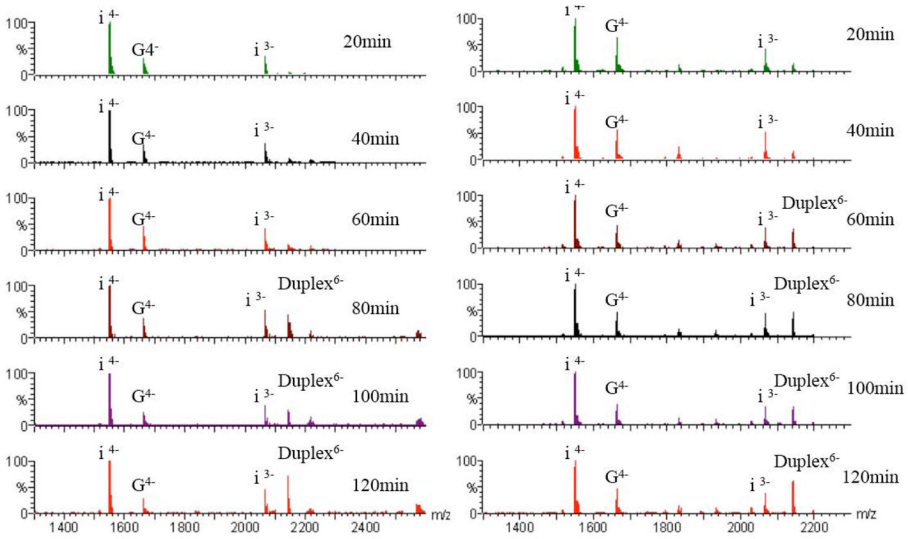

Fig. 3.

ESI-MS spectra comparison between **32** and TMPyP4. Left: ESI-MS spectra of a mixture of 5μM G-DNA, 5μM **32**, and 5μM C-DNA at different time; Right: ESI-MS spectra of a mixture of 5μM G-DNA, 5μM TMPyP4, and 5μM C-DNA at the times indicated.

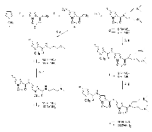

Scheme 1a.

[a] Reagents and conditions: (a) trichloroacetyl chloride, ether, 0 °C to room temperature; (b) HNO_3 (fuming), acetyl anhydride, −40 °C to room temperature; (c) **5** $NH[(CH_2)_3N(CH_3)_2]_2$ or **4** $NH_2(CH_2)_3N(CH_3)_2$, THF, room temperature; (d) Pd/C, H_2 (37psi), MeOH, room temperature; (e) **3**, THF, room temperature; (f) Pd/C, H_2 (37psi), MeOH, room temperature; (g) **3**, THF, room temperature; (h) Pd/C, H_2 (37psi), MeOH, room temperature; (i) Pd/C, H_2 (37psi), MeOH, room temperature; (j) Pd/C, H_2 (37psi), MeOH, room temperature.

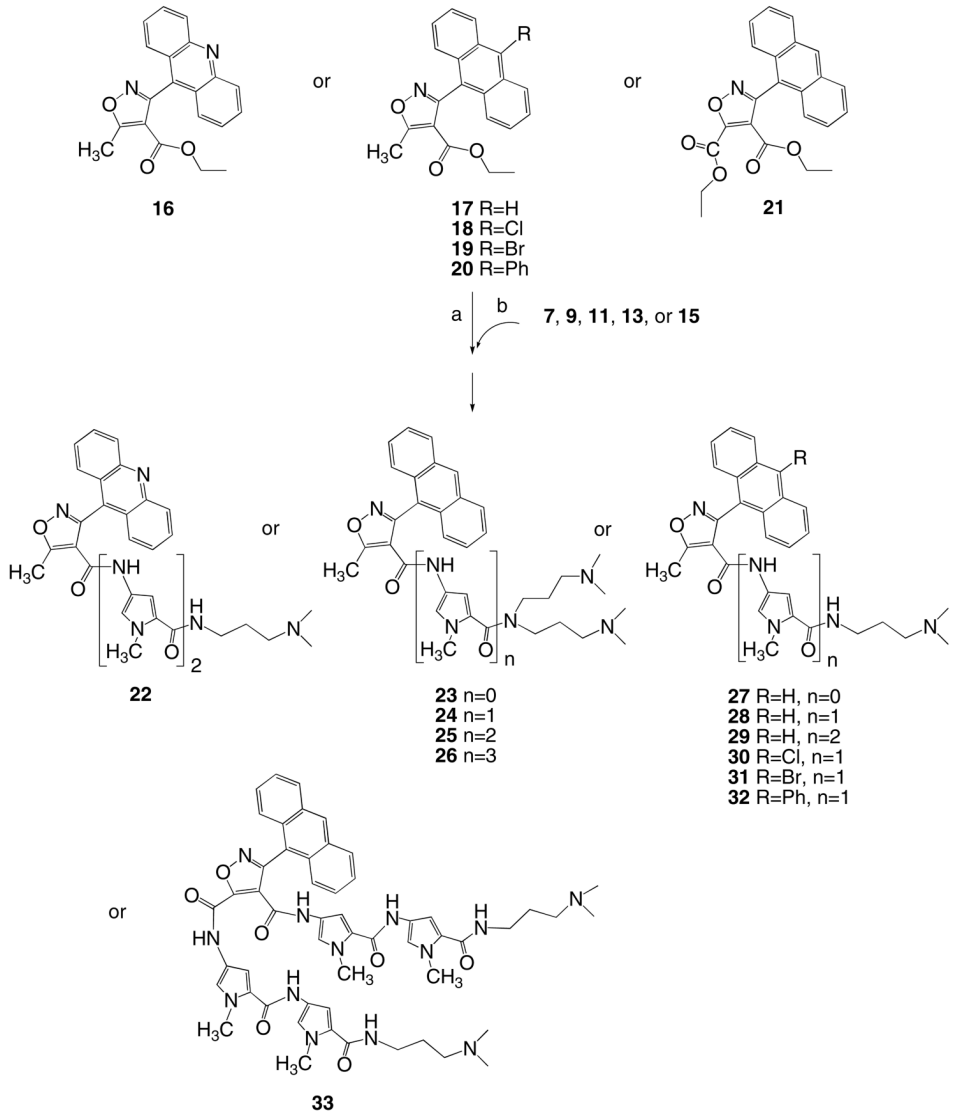

Scheme 2a.

[a] Reagents and conditions: (a) $SmCl_3$ (10%), THF, room temperature, 2h; (b) $Al(CH_3)_3$ (1 equiv.), THF, 0 °C to room temperature, 1h; (c) THF, reflux, 36 hours.

Table 1

Synopsis of *in vitro* antitumor activities of compounds (**22–33**) against the NCI-DTP 60 cell line screen. The full 60 cell line data is available free of charge on the internet at the NCI-DTP site [http://dtp.nci.nih.gov/index.html]. NSC numbers are provided for each compound in this table in the Supporting information.

AIM Compound	−Log (mean GI_{50})[a]	Mean GI_{50} (μM)	N[b]	Efficacy[c]
16	4.69	20.4	2	
22	4.68	20.9	0	
23	5.31 – 5.34	4.90 – 4.57	37 – 42	Non-small cell lung cancer EKVX: 6.18, colon cancer HCC-2998: 6.11, CNS cancer SF-295: 7.52
24	5.41	3.89	44	
25	4.81	15.5	7	
26	4.61	24.5	0	
27	4.49	32.4	1	Non-small cell lung cancer NCI-H226: <8.00
28	5.10	7.94	23	Non-small cell lung cancer HOP-62: 6.39
29	4.91 – 4.98	12.3 – 10.5	12 – 14	
30	5.72 – 5.75	1.91 – 1.78	53– 57	Non-small cell lung cancer HOP-92: 7.03
31	5.06	8.71	18	CNS cancer SNB-75: 6.80
32	5.71 – 6.04	1.95 – 0.91	60	CNS cancer SF-539: <8.00, Non-small cell long cancer HOP-62: 7.98, HOP-92: 7.2
33	4.69	20.4	2	

[a] Range given for those compounds selected for a second screening by NCI's Biological Evaluation Committee.

[b] The number of cell lines inhibited at single digit micromolar

[c] Cell lines inhibited in the nanomolar range, with -Log GI_{50}.

Table 2

COMPARE Analysis using **29**, NSC D-694332, as “seed”

Antitumor Agent	PCC	Mechanism
Tetrandrine	0.517	Calcium Channel Blocker
Macbecin II	0.488	DNA anti-metabolite
Didemnin B	0.468	Inhibits Ribosomal Protein Synthesis
Tetrocarcin A	0.462	Modulates Mitochondrial Apoptosis
Spirogermanium	0.459	Alkylating Agent
Pibenzimol	0.453	Minor Groove Binder
Thalicarpine	0.450	Unknown
Neocarzinostatin	0.436	Enediyne Strand Breaker
Fostriecin	0.421	Topo II Catalytic Inhibitor
Emofolin Sodium	0.415	DHFR inhibitor
Vinblastin Sulfate	0.414	Antimitotic Agent

Table 3

Energy calculation of rotation toward isoxazole/anthracene coplanarity

Energy Difference From 90°	
Angle(degrees)	**Energy (Kcal)**
120.14	6.96
121.44	7.87
122.24	8.82
123.44	10.46
124.24	11.73
125.44	13.96
126.24	15.70
127.44	18.76
128.24	21.16
129.34	25.03
130.54	30.19
131.34	35.08
132.54	42.40
133.44	48.40
134.24	65.10
135.44	68.00